

that DNAJB8 is a novel cancer-testis (CT) antigen and also a novel CSC antigen. DNAJB8 has a role in the maintenance of RCC CSCs/CICs. We compared the potency of DNAJB8 as an immunologic target with that of Survivin, which is expressed in both CSC/CIC and non-CSC/CIC populations (shared antigen), and we found that DNAJB8 is more effective than Survivin. Our results suggest that targeting a CSC antigen is more effective than targeting a shared antigen and that DNAJB8 is a candidate for CSC/CIC-targeting immunotherapy.

Materials and Methods

Cell lines

RCC cell lines ACHN, Caki-1, SMKTR2, and SMKTR3 and the murine RCC cell line RenCa of BALB/c mouse origin were maintained in RPMI 1640 (Sigma) supplemented with 10% FBS. HEK293T cells and the murine fibroblast cell line BALB/3T3 of BALB/c mouse origin were grown in Dulbecco's Modified Eagle's Medium (DMEM; Sigma) supplemented with 10% FBS. PLAT-E and PLAT-A cells (kind gifts from Dr. T. Kitamura, Division of Stem Cell Signaling, The Institute of Medical Science, The University of Tokyo, 4-6-1 Shirokanedai, Minato-ku, Tokyo 108-8639, Japan) were grown in DMEM supplemented with 10% FBS, 10 μ g/mL blasticidin, and 1 μ g/mL puromycin.

Mice

All mouse procedures were carried out in accordance with institutional protocol guidelines at Sapporo Medical University School of Medicine. BALB/c female mice were purchased from Clea Japan and nonobese diabetic/severe combined immunodeficient (NOD/SCID) mice were purchased from Charles River Laboratory Japan at the age of 6 to 8 weeks.

Reverse transcriptase PCR analysis

Reverse transcriptase PCR (RT-PCR) analysis was carried out as described previously (18). Human Multiple Tissue cDNA Panels I and II (Clontech) were used as templates of normal adult tissue cDNAs. Except for *SOX2* and *Sox2*, PCR amplification was done in 20 μ L of PCR mixture containing 0.25 μ L of the cDNA mixture, 0.1 μ L of Taq DNA polymerase (Qiagen), and 12 pmol of primers. The PCR mixture was initially incubated at 94°C for 2 minutes, followed by 35 cycles of denaturation at 94°C for 15 seconds, annealing at 58°C for 30 seconds, and extension at 72°C for 30 seconds. PCR amplification of *SOX2* and *Sox2* was carried out in 20 μ L of PCR mixture containing 0.4 μ L of the cDNA mixture, 0.2 μ L of PrimeSTAR HS DNA polymerase (Takara), and 12 pmol of primers. The PCR mixture was initially incubated at 94°C for 2 minutes, followed by 35 cycles of denaturation at 94°C for 15 seconds and annealing and extension at 68°C for 30 seconds. Primers used in experiments are summarized in Supplementary Table.

Development of anti-DNAJB8 monoclonal antibody and Western blot analysis

A monoclonal antibody (mAb) against DNAJB8 (clone #EMR-DNAJB8.214-8) was generated, as described previously (19), by immunizing mice 4 times weekly with recombinant His-tag DNAJB8 protein produced and purified by a Ni-NTA

agarose column (Qiagen). Cell lysate with SDS sample buffer was separated by denaturing SDS-PAGE. Separated proteins were transferred onto nitrocellulose membranes and probed with mouse anti-FLAG M2 antibody (Sigma) or anti-DNAJB8 antibody. β -Actin was used as a loading control and was detected with a mouse mAb (Sigma). Anti-DNAJB8 antibody was used at 200 times dilution. Anti-FLAG antibody and anti- β -actin antibodies were used at 2,000 times dilution.

Side population analysis

Side population (SP) cells were isolated as described previously using Hoechst 33342 dye (Lonza) with some modifications (20). Briefly, cells were resuspended at 1×10^6 /mL in prewarmed DMEM supplemented with 5% FBS. Hoechst 33342 dye was added at a final concentration of 2.5 μ g/mL in the presence or absence of verapamil (50 μ mol/L; Sigma-Aldrich), and the cells were incubated at 37°C for 90 minutes with intermittent shaking. Analyses and sorting were carried out with an FACS Aria II cell sorter (Becton Dickinson).

Retroviral gene transduction and generation of stable transformants

Transduction of genes into cells was carried out by a retrovirus-mediated method as described previously (21). PLAT-A and PLAT-E cells, which are amphotropic and ecotropic packaging cells, respectively, were transiently transduced with a pMXs-puro (kind gift from Dr. T. Kitamura, Tokyo, Japan) retroviral vector expressing FLAG-tagged DNAJB8, Dnajb8, and Survivin, V5-tagged DNAJB8 Δ SSF-SST mutant, and a control plasmid using FuGENE HD transfection reagent (Roche) following the manufacturer's protocol. Retroviral supernatants were harvested 48 hours after transfection. The supernatant was used for infection of BALB/3T3 cells, ACHN cells, or RenCa cells in the presence of 8 μ g/mL of polybrene (Sigma) overnight. For the generation of stable transformants, the infected cells were selected with 1 μ g/mL puromycin. DNAJB8, Dnajb8, or Survivin expression was confirmed by Western blot analysis.

siRNA-mediated knockdown

DNAJB8 siRNAs (HSS136480, HSS136482, and HSS176060) were purchased from Invitrogen and transfected using Lipofectamine RNAi MAX reagent (Invitrogen) according to the protocol of the manufacturer. Cells were transfected with siRNA 72 hours before analysis. Nontargeting siRNA (Stealth RNAi Negative Control; Invitrogen) was used as a negative control. DNAJB8 knockdown was confirmed by Western blot analysis.

Site-directed mutagenesis

Plasmids including the target site for mutation as a template and primers that contain the desired mutation encoding the same amino acids as those of the wild-type sequence were used for site-directed mutagenesis. The sequences of primers are listed in Supplementary Table. Mutated plasmids were generated by 20 cycles of PCR amplification with KOD plus DNA polymerase (TOYOBO) and then digested by restriction enzyme *DpnI* for 2 hours. The generated nicked dsDNA was transformed into BL21

strain of *Escherichia coli* and amplified. The mutations were verified by DNA sequencing.

Xenograft transplantation

Sorted SP and non-SP cells, and gene-transfected ACHN cells were injected into the subcutaneous space of the back of syngeneic BALB/c mice (for RenCa cells) or NOD/SCID mice (for ACHN cells). Tumor growth was monitored weekly, and tumor volume was calculated by $XY^2/2$ (X = long axis, Y = short axis).

DNA vaccine constructs

Murine *Dnajb8* and *Survivin* cDNAs were amplified by PCR from RenCa cells and subcloned into *Bam*HI and *Xho*I cloning sites of the modified pcDNA3.1(+) vector (Invitrogen), which contains the murine immunoglobulin kappa chain signal sequence at the N terminus [inserted into *Nhe*I and *Hind*III cloning sites of pcDNA3.1(+)] and a FLAG epitope at the C terminus [inserted into *Xba*I and *Pme*I cloning sites of pcDNA3.1(+)] of the expression antigen. A blank vector, modified pcDNA3.1(+), was used as control. The sense sequences and antisense sequences of the inserted oligo DNA are listed in Supplementary Table.

In vitro stimulation of CD8⁺ T cells

One week after the DNA vaccination, mice were sacrificed and a single-cell suspension was prepared from the spleen. Erythrocytes were lysed by osmotic shock (0.1 mol/L NH₄Cl), and CD8⁺ T cells were isolated from splenocytes by using a MACS separation system (Miltenyi Biotech). A total of 5×10^6 CD8⁺ or CD8⁻ cells per well were, respectively, seeded in a 24-well plate with RPMI-1640 medium (Sigma) supplemented with 10% FBS. Phytohemagglutinin (PHA) blasts were generated from CD8⁻ cells by using 50 IU/mL IL-2 and 2 μ g/mL PHA for 3 days, and then *Dnajb8* or *Survivin* genes were transduced with a retrovirus vector. On day 7, 5×10^5 *Dnajb8*- or *Survivin*-expressing PHA blasts were irradiated (100 Gy), washed once, and added onto CD8⁺ cells. On day 8, IL-2 was added to each well at a concentration of 50 IU/mL. On day 14, the antigen-specific IFN- γ release of CD8⁺ T cells was assessed by an ELISPOT assay as described previously (19).

Tumor growth inhibition assay and rechallenge study

To measure protective immunity, BALB/c female mice were weekly immunized with DNA plasmid 4 times by injection into their footpad followed by injection of 1×10^5 RenCa tumor cells. Tumor growth was monitored weekly. RenCa/*Dnajb8* cells (1×10^6) were injected subcutaneously into the back of BALB/c female mice that had rejected a previous injection of 1×10^5 RenCa cells.

In vivo depletion of T-cell subsets

Mice were injected intraperitoneally with 500 μ g of either anti-CD4 (clone: GK L5, rat IgG) or anti-CD8 (clone: 2.43, rat IgG) mAb 2 days before immunization and then immunized with cDNA plasmid vaccines once weekly for 4 weeks. Tumor cells were challenged 1 week after the fourth immunization.

Depletion of CD4⁺ and CD8⁻ T cells was verified by flow cytometry.

Statistical analysis

Data are presented as means \pm SD. Differences in variables were assessed using Student *t* test. Survival curves were constructed according to the Kaplan–Meier method. Statistical significance was determined by the log-rank test. $P < 0.05$ was considered significant. Statistical analysis was done with Stat Mate III (ATMS Co., Ltd.).

Results

DNAJB8 is a potential cancer-testis antigen

DNAJB8 has been reported to inhibit the aggregation of misfolding proteins and to protect cells from cell death (22); however, its role in cancer cells is not clear. We first investigated *DNAJB8* mRNA distributions in human normal adult tissues and cancer cells by RT-PCR. *DNAJB8* mRNA is barely expressed in normal mature tissues except for the testis (Fig. 1A), and it is expressed in all cells of human cancer lines (Fig. 1B).

We generated a DNAJB8-specific mAb (clone: #EMR-DNAJB8.214-8) to investigate DNAJB8 protein expression. The mAb #EMR-DNAJB8.214-8 showed DNAJB8-specific reaction using FLAG-tagged DNAJB8-overexpressed ACHN cells by Western blotting (Fig. 1C). Interestingly, the mAb #EMR-DNAJB8.214-8 was also reactive for FLAG-tagged mouse *Dnajb8*-transduced RenCa cells (Fig. 1C). Therefore, the mAb #EMR-DNAJB8.214-8 is reactive for both human DNAJB8 and mouse DNAJB8 proteins. DNAJB8 proteins were detectable in human sperm and mice testis tissues (Fig. 1D). Immunohistochemical staining also confirmed protein expression in human testis and mouse testis. Matured sperm and spermatid were positive for #EMR-DNAJB8.214-8, whereas spermatogonia and spermatocytes were negative for #EMR-DNAJB8.214-8 (Fig. 1E). DNAJB8 protein was also detectable in human RCC (clear cell carcinoma) tissues, whereas it was undetectable in counterpart human renal tubules (Fig. 1F). These expression profiles strongly indicated that DNAJB8 is a novel cancer-testis antigen (23).

Isolation and analysis of RCC stem-like population from human and mouse RCC cells

To address DNAJB8 functions in RCC CSCs/CICs, we carried out SP analysis using the human RCC cell lines ACHN, Caki1, SMKTR2, and SMKTR3 and the mouse RCC cell line RenCa. SP cells were detectable in ACHN, Caki1, and RenCa cells, and those SP cells were completely inhibited by verapamil (Fig. 2A and Supplementary Fig. S1), indicating that SP cells were specific for ABC transporter activity. The ratios of SP cells in ACHN, Caki1, and RenCa cells were 2.6%, 0.2%, and 18%, respectively. The ratios of SP cells in Caki1, SMKTR2, and SMKTR3 cells were too low for further analysis, and we therefore used ACHN and RenCa in the following experiments. It has been shown that SP cells were not enriched with CSCs/CICs in some types of cancer cells (24), and thus it is essential to validate that SP cells are enriched with CSCs/CICs. ACHN SP cells initiated tumor formation with 10^3 cells, whereas ACHN

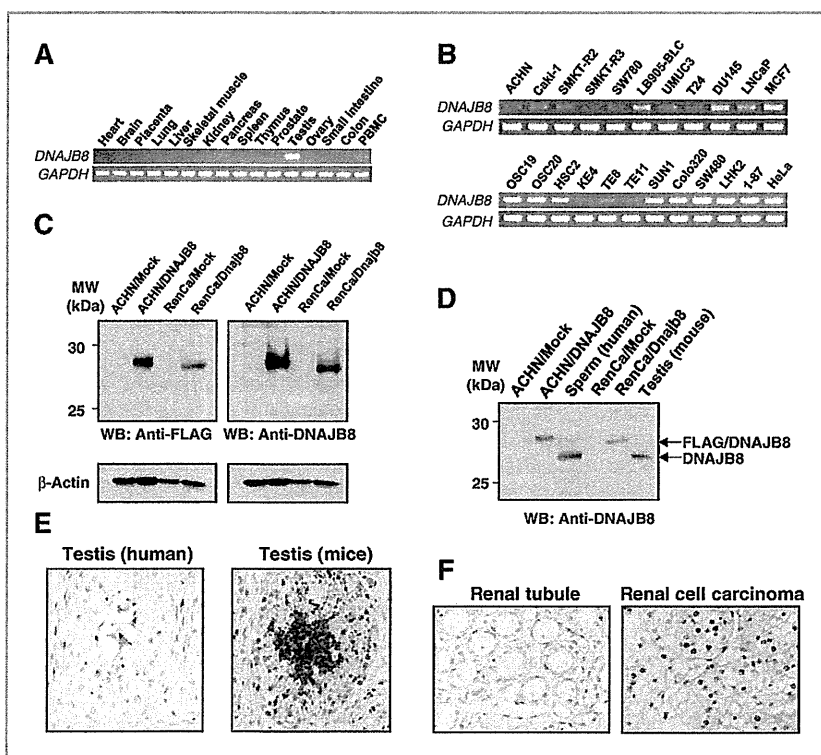


Figure 1. Expression of DNAJB8. **A**, RT-PCR analysis with normal organs. Expression of *DNAJB8* mRNA was examined by RT-PCR. *GAPDH* was used as a positive control. **B**, RT-PCR analysis with cancer cells. Expression of *DNAJB8* mRNA was examined by RT-PCR. *GAPDH* was used as a positive control. **C**, Western blot analysis. DNAJB8-transduced ACHN cells and Dnajb8-transduced RenCa cells were analyzed with anti-FLAG antibody and anti-DNAJB8 mAb (clone: #EMR-DNAJB8.214-8). ACHN/DNAJB8 and RenCa/Dnajb8 represent ACHN and RenCa cells transduced with FLAG-tagged DNAJB8 and Dnajb8, respectively. **D**, Western blot analysis. Endogenous DNAJB8 protein expression was addressed in human sperm and mouse testis using anti-DNAJB8 mAb (#EMR-DNAJB8.214-8). ACHN/DNAJB8 and RenCa/Dnajb8 were used as positive controls. **E**, immunohistochemical staining of human testis and mouse testis. Human testis and mouse testis tissues were stained with mAb #EMR-DNAJB8.214-8. Magnification, $\times 200$. **F**, immunohistochemical staining of human normal kidney and RCC. Human normal kidney and RCC (clear cell carcinoma) tissues were stained with mAb #EMR-DNAJB8.214-8. Magnification, $\times 200$. *GAPDH*, glyceraldehyde-3-phosphate dehydrogenase; WB, Western blot.

main population (MP) cells needed 10^1 cells to initiate tumor formation (Fig. 2B and Table 1). RenCa SP cells initiated tumor formation with 10^2 cells, whereas RenCa MP cells needed 10^3 cells to initiate tumor formation (Fig. 2B and Table 1). These data indicated that SP cells derived from ACHN and RenCa cells were enriched with CSCs/CICs.

We carried out RT-PCR analysis to evaluate genetic characteristics of SP and MP cells derived from ACHN and RenCa cells (Fig. 2C). SP cells derived from ACHN and RenCa cells showed higher expression levels of *SOX2/Sox2* and *POU5F1/Pou5f1* than did MP cells, indicating that they present stem cell-like phenotypes (Fig. 2C). Recently, induction of epithelial to mesenchymal transition (EMT) in transformed mammary epithelial cells has been shown to result in the creation of populations of cells that are highly enriched in CSCs/CICs (25); therefore, we analyzed EMT-related gene expression in SP and MP cells. Both ACHN and RenCa SP cells showed repressed *CDH1/Cdh1* expression. ACHN SP cells preferentially expressed *SNAI2* and RenCa SP cells preferentially expressed *Snail* and *Twist1*, representative EMT-inducing transcription

factors. These findings suggested that SP cells of RCC are enriched with CSCs/CICs and have a partial EMT feature.

DNAJB8/Dnajb8 mRNA was predominantly expressed in SP cells derived from both ACHN and RenCa cells (Fig. 2D). DNAJB8 mRNA was also predominantly expressed in SP cells derived from colon carcinoma cells (KM12LM and SW480 cells), lung carcinoma cells (LHK2 cells), and breast carcinoma cells (MCF7 cells; Supplementary Fig. S2). Western blotting and immunostaining using SP cells and MP cells derived from ACHN and RenCa cells also revealed preferential expression of DNAJB8 protein in SP cells (Fig. 2E and F and Supplementary Fig. S3A and B). DNAJB8 protein was also preferentially expressed in SP cells derived from LHK2 and SW480 cells (Supplementary Fig. S4). These findings indicated that DNAJB8/Dnajb8 is preferentially expressed in the CSC/CIC population and that DNAJB8 is therefore a novel CSC antigen.

DNAJB8 function in maintenance of CSCs/CICs

To address the functions of DNAJB8 in RCC CSCs/CICs, we generated stable transformants expressing DNAJB8 (Fig. 1C).

Nishizawa et al.

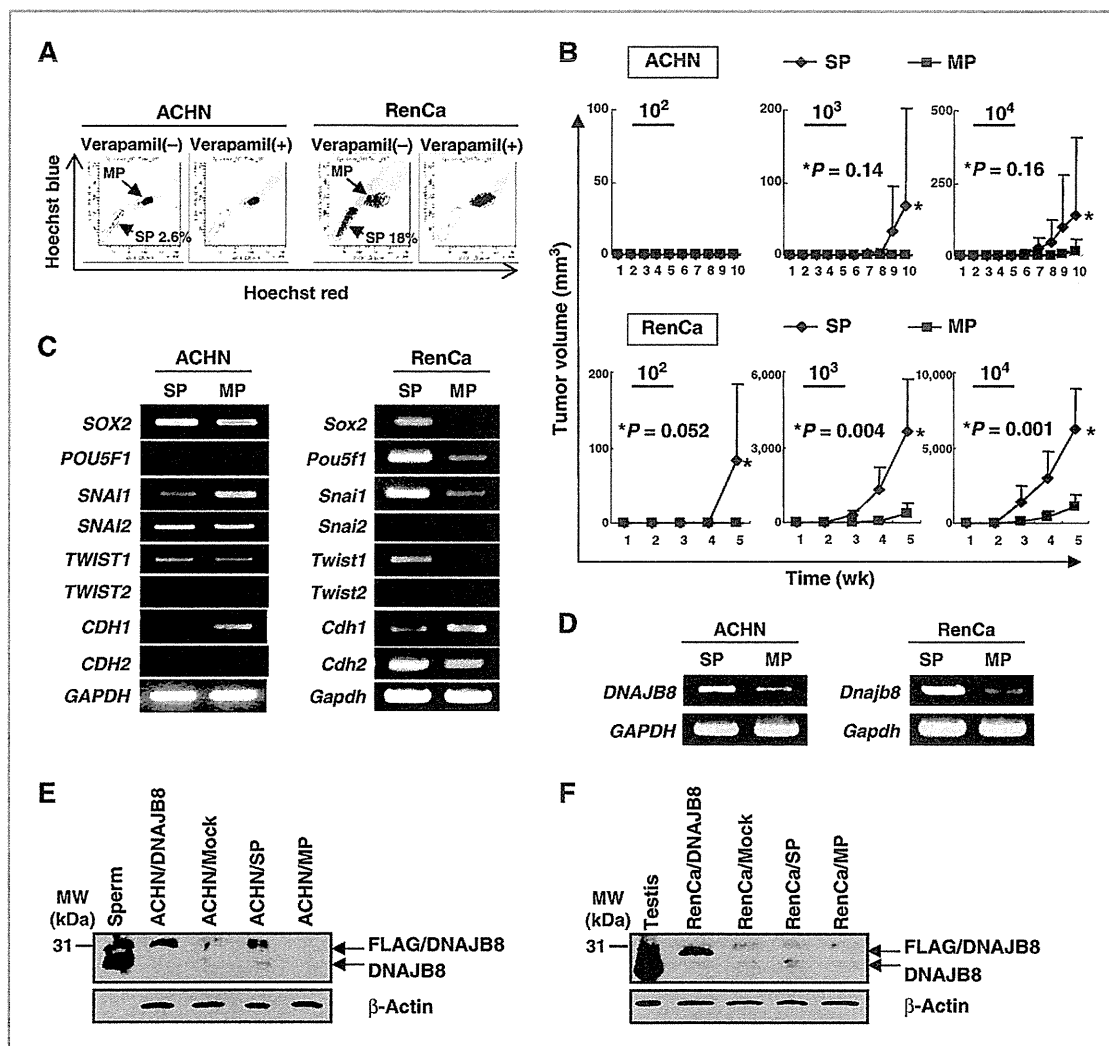


Figure 2. Isolation of CSCs/CICs from human and mouse RCC cells. **A**, SP analysis. ACHN human RCC cells and RenCa mouse RCC cells were stained with Hoechst 33342 dye with or without verapamil and analyzed with an FACSARIA II cells sorter. The percentages represent the ratios of SP cells. **B**, tumor-initiating ability. SP cells and MP cells (10^2 – 10^4 cells) derived from ACHN cells were injected into NOD/SCID mice and tumor growth was observed. Data are means \pm SD. **C**, RT-PCR analysis. SP and MP cells derived from ACHN and RenCa cells were analyzed by RT-PCR. *GAPDH* was used as a positive control. **D**, RT-PCR analysis. SP and MP cells were derived from ACHN, and RenCa cells were examined for expression of *DNAJB8* and *Dnajb8*, respectively. *GAPDH* was used as a positive control. **E**, Western blot analysis. Expression of DNAJB8 proteins in human sperm, in ACHN/DNAJB8 and ACHN/Mock cells, and in SP and MP cells derived from ACHN cells was detected by Western blotting using anti-DNAJB8 mAb #EMR-DNAJB8.214-8. **F**, Western blot analysis. Expression of DNAJB8 proteins in the mouse testis, in RenCa/Dnajb8 and RenCa/Mock cells, and in SP and MP cells derived from RenCa cells was detected by Western blotting using anti-DNAJB8 mAb #EMR-DNAJB8.214-8.

The percentages of SP cells in DNAJB8-transduced ACHN and RenCa cells (ACHN/DNAJB8 and RenCa/DNAJB8) were increased compared with those in control cells (ACHN/Mock and RenCa/Mock cells; Fig. 3A). Similar phenomena were observed in several other cell lines including RCC (Caki1), prostate carcinomas (LNCaP and DU145), and bladder carcinoma cells (T-24; Supplementary Fig. S5). Furthermore, DNAJB8-transduced ACHN cells showed higher tumor-initiat-

ing ability than that of Mock-transduced ACHN cells (Fig. 3B and Table 1). DNAJB8 contains an N-terminal J-domain, which is responsible for association with HSP70 families, and a C-terminal serine-rich region, which is capable of interacting with histone deacetylases (HDAC; HDAC4, HDAC6, and SIRT2) and has a role in suppression of protein aggregation. A DNAJB8 mutant that lacks the C-terminal serine-rich region (Δ SSF-SST) showed a smaller SP augmentation effect (Supplementary Fig.

Table 1. Tumor-initiating ability of RCCs

Cells		Tumor initiation (injected cell number) ^a			
		10	10 ²	10 ³	10 ⁴
ACHN	SP cells	n.d.	0/5	3/6	4/6
	MP cells	n.d.	0/5	0/6	1/6
RenCa	SP cells	0/5	3/5	5/5	5/5
	MP cells	0/5	0/5	5/5	5/5
ACHN	DNAJB8 transduced	n.d.	0/5	3/5	9/9
	Mock transduced	n.d.	0/5	0/5	7/9
ACHN/DNAJB8	SP cells	n.d.	0/4	2/2	n.d.
	MP cells	n.d.	0/4	0/2	n.d.

Abbreviation: n.d., not determined.

^aThe tumor-initiating abilities were evaluated at day 70 postcell injection for ACHN cells and at day 35 for RenCa cells.

S6), suggesting that the C-terminal serine-rich region has a role in the induction of CSCs/CICs.

DNAJB8 gene knockdown experiments were carried out using gene-specific siRNAs. Three different *DNAJB8*-specific siRNAs (siRNA A, B, and C) could suppress the expression of *DNAJB8* (Fig. 3C); therefore, we used siRNA A in the following experiments. Transfection of siRNA A almost completely eliminated the SP cell population in both wild-type ACHN and ACHN/DNAJB8 cells (Fig. 3D). Furthermore, siRNA A transfection significantly inhibited the tumorigenicity of ACHN cells in NOD/SCID mice (Fig. 3E). Gene knockdown of *DNAJB8* by siRNA transfection almost completely decreased the numbers of SP cells. Thus, we generated a *DNAJB8* mutant (*DNAJB8* mt) by site-directed mutagenesis to confirm the siRNA results (Fig. 3F). *DNAJB8* mt contains 6 DNA point mutations within the siRNA target sequence and codes the same amino acid sequence as that of the wild type. *DNAJB8* mt was insensitive to siRNA A transfection, whereas *DNAJB8* wt was inhibited by siRNA transfection (Fig. 3G). The siRNA transfection into ACHN/*DNAJB8* cells decreased the numbers of SP cells (Fig. 4D); however, the *DNAJB8* mt stable transformant showed no reduction of SP cells by siRNA transfection (Fig. 3H). These results indicated that the effects of siRNA transfection were specific for targeting *DNAJB8* mRNA, and *DNAJB8* therefore has a role in the maintenance of RCC CSCs/CICs.

DNAJB8-targeting immunotherapy

Because *DNAJB8* is one of the cancer-testis antigens and one of the CSC antigens and has a role in the maintenance of RCC CSCs/CICs, we hypothesized that *DNAJB8* is a suitable immunologic target of RCC CSCs/CICs-targeting immunotherapy. However, it is not clear which will bring about a better antitumor effect: targeting CSC antigens or targeting shared antigens. On the basis of this point of view, we compared the immunogenicity of *DNAJB8* with that of the well-characterized TAA Survivin (26–29), as Survivin is expressed in both CSCs/CICs and non-CSCs/CICs at the same levels (Fig. 5A) and it is a shared antigen.

We subcloned FLAG-tagged *Dnajb8* and Survivin into the pcDNA3.1 expression vector and confirmed the expression by Western blot analysis (Fig. 4B). We carried out an ELISPOT assay to verify the immunization of DNA vaccine. Anti-*Dnajb8*- or anti-Survivin-specific IFN- γ spots could be observed with CD8⁺ T cells derived from *Dnajb8*- or Survivin-immunized mice, respectively (Fig. 4C). To address the antitumor effects, we injected RenCa cells into *Dnajb8*- and Survivin-immunized mice. Antitumor effects were observed in both *Dnajb8*- and Survivin-immunized mice compared with control vector- or PBS-immunized mice (Fig. 4D; *P* values of 0.002 and 0.026, respectively). *Dnajb8*-immunized mouse showed significantly greater antitumor effect than that in Survivin-immunized mouse (*P* = 0.03; Fig. 4D).

To evaluate the subtype of T cells for antitumor activities, we depleted murine CD4⁺ or CD8⁺ T cells in immunized mice by 4 intraperitoneal injections of anti-CD4 or CD8 antibody (Fig. 5A). CD4⁺ T-cell depletion significantly inhibited the antitumor effect of *Dnajb8* immunization (*P* = 0.046), whereas CD8⁺ T-cell depletion did not (Fig. 5B). However, the survival period of RenCa cell-injected mice was significantly shorter for both CD4⁺ T-cell-depleted mice and CD8⁺ T-cell-depleted mice than the survival period of *Dnajb8*-immunized mice (Fig. 5C). These observations indicated that both CD8⁺ T cells and CD4⁺ T cells might have a role in the antitumor effect. Three of 5 *Dnajb8*-immunized mice showed complete inhibition of tumor formation initiation, and the mice were therefore rechallenged with 10 times larger numbers of higher tumorigenic RenCa/*DNAJB8* cells. Initiation of tumor formation was completely inhibited in those mice, suggesting a strong tumor-inhibitory effect of *Dnajb8* immunization (Fig. 5D).

Discussion

In this study, we investigated the distributions of *DNAJB8* mRNA and protein and found that *DNAJB8* is expressed only in the testis among normal tissues. *DNAJB8* protein expression was detected in postmeiotic sperm and spermatid. Previous studies have shown that *DNAJB6*, *DNAJB1*, and *DNAJB13* are also expressed in the testis (30–32), and *Dnaja1* was reported to

Nishizawa et al.

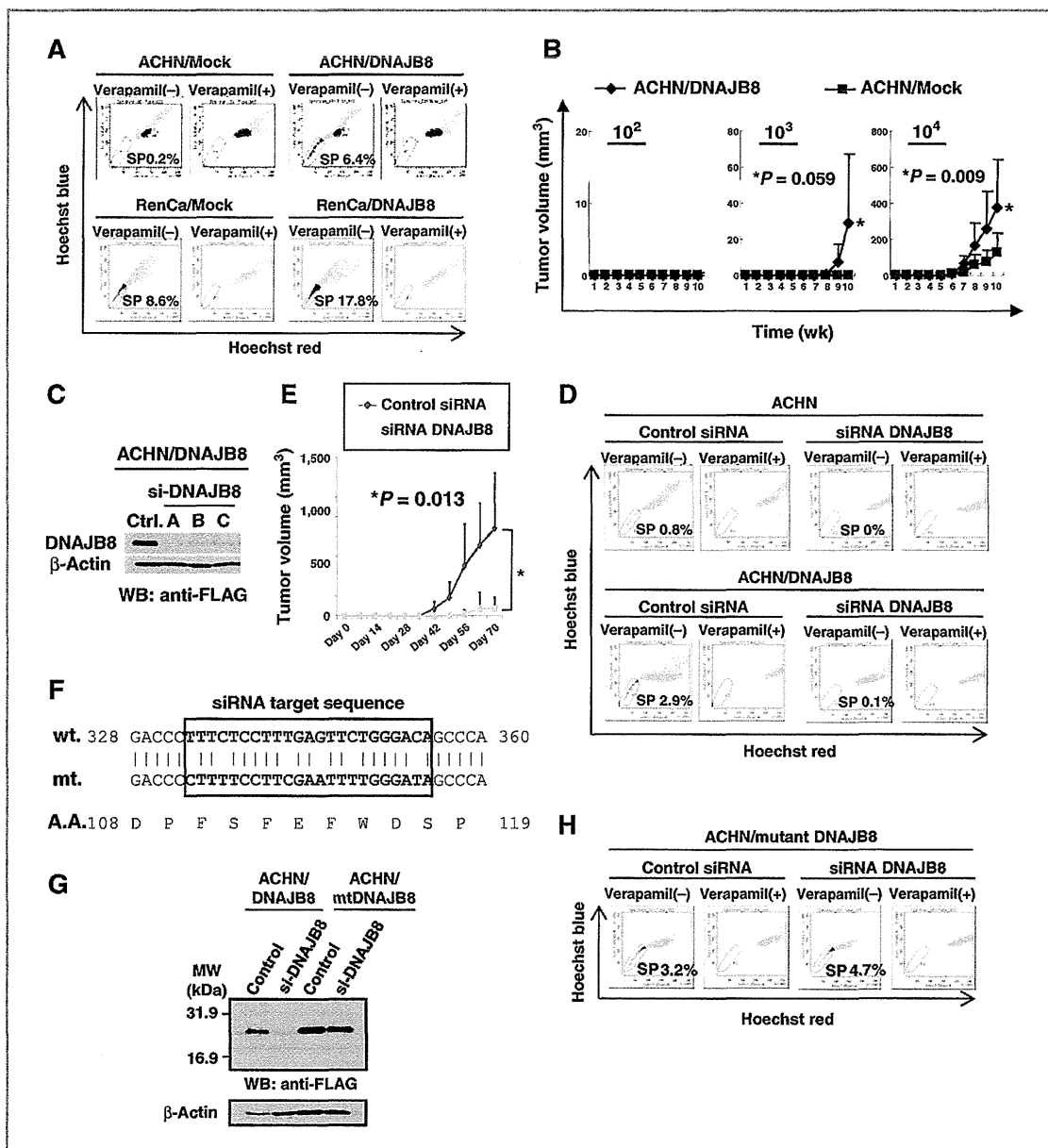


Figure 3. DNAJB8 function in maintenance of RCC CSCs/CICs. A, SP analysis of DNAJB8-transduced RCC cells. DNAJB8-transduced ACHN cells (ACHN/DNAJB8) and Dnajb8-transduced RenCa cells (RenCa/DNAJB8) were analyzed for SP cells. Mock-transduced ACHN and RenCa cells were used as controls (ACHN/Mock and RenCa Mock). The percentages represent the ratios of SP cells. B, tumor-initiating ability of ACHN/Mock cells and ACHN/DNAJB8 cells. ACHN/Mock cells and ACHN/DNAJB8 cells (10^2 - 10^4 cells) were injected into NOD/SCID mice. Data are means + SD. C, Western blot analysis of DNAJB8-specific siRNA-transduced ACHN/DNAJB8 cells. ACHN/DNAJB8 cells were transfected with 3 different siRNAs specific for DNAJB8 (siRNA A, B, and C). Two days after transfection, ACHN/DNAJB8 cells were analyzed by Western blotting using anti-FLAG mAb. D, SP analysis of DNAJB8-knockdown RCC cells. ACHN and ACHN/DNAJB8 cells were transfected with DNAJB8-specific siRNA A. Two days after siRNA transfection, cells were analyzed for SP cells. The percentages represent the ratios of SP cells. E, tumor-initiating ability of DNAJB8-knockdown RCC cells. DNAJB8-specific siRNA or control siRNA was transfected into ACHN cells. Two days after transfection, cells were injected into NOD/SCID mice. Data are means + SD. F, DNAJB8-mutant sequence. DNAJB8-mutant (mt) gene was constructed by site-directed PCR. The square indicates siRNA target sequence. Numbers indicate DNA sequence and amino acid sequence, respectively. G, Western blotting of mt DNAJB8. DNAJB8 siRNA was transfected into ACHN/DNAJB8 and ACHN/DNAJB8 mt cells. Expression of DNAJB8 was evaluated by Western blotting using anti-FLAG mAb. H, canceling test. DNAJB8-siRNA-transduced ACHN/DNAJB8 mt cells were analyzed for SP cells. The percentages represent the ratios of SP cell.

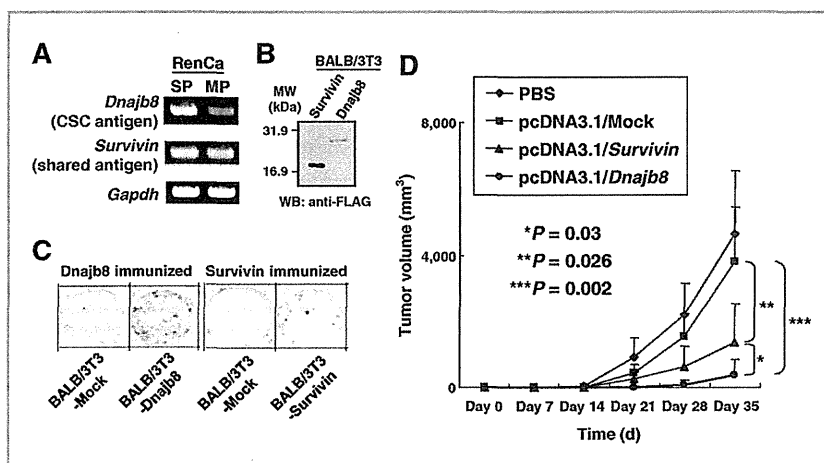


Figure 4. Immunogenicity of DNAJB8. A, RT-PCR analysis. SP and MP cells derived from RenCa cells were analyzed for expression of *Dnajb8* (CSC antigen) and *Survivin* (shared antigen) by RT-PCR. *Gapdh* was used as a positive control. B, Western blot analysis using Dnajb8- and Survivin-transduced BALB/3T3 cells. Dnajb8- or Survivin-transduced BALB/3T3 cells were analyzed by Western blotting using anti-FLAG mAb. C, immunoreactions to Dnajb8 and Survivin. Spleen cells were isolated from mice immunized with Dnajb8 plasmid or Survivin plasmid. Spleen cells were stimulated *in vitro* and then immunoreactivity to Dnajb8 or Survivin was evaluated by an ELISPOT assay using Dnajb8-transduced BALB/3T3 (BALB/3T3/Dnajb8) cells and Survivin-transduced BALB/3T3 (BALB/3T3/Survivin) cells. D, antitumor effect of DNA vaccine. Dnajb8, Survivin, Mock plasmid, and PBS-immunized mice were challenged with RenCa cells by injecting 1×10^5 RenCa cells subcutaneously. Data are means \pm SD.

have a role in spermatogenesis by regulating androgen receptor signals (33). Therefore, DNAJB8 is another testis-expressing HSP40 family protein and may have a role in spermatogenesis, especially in the postmeiotic stage.

We isolated RCC CSCs/CICs as SP cells. SP cells have been reported to be enriched with CSCs/CICs in several kinds of malignancies (34–36). SP cells derived from RCC and normal renal tubule epithelia have also been reported (37, 38); however, the tumor-initiating ability of those RCC SP cells has not been characterized yet. Tumor-initiating ability is one of major characteristics of CSCs/CICs, and this characteristic makes CSCs/CICs a reasonable target of cancer therapy. In this study, SP cells derived from ACHN human RCC cells and RenCa mouse RCC cells showed higher tumor-initiating ability than that of MP cells, and these SP cells are suitable for analysis of RCC CSCs/CICs.

HSPs, especially HSP90, are overexpressed in a wide range of human cancers, allowing mutant proteins to be retained in cancer cells and to confer resistance to cytotoxic therapies (39). On the other hand, most of the HSP40 family proteins have been reported to be inversely correlated with high-grade malignancy, and HSP40 family proteins have been reported to function as tumor suppressors (40). In this study, we found that DNAJB8 was expressed in several kinds of cancer cells, including RCCs, and that it was preferentially expressed in the CSC/CIC population. DNAJB8 has a role in maintenance of RCC CSCs/CICs as shown by siRNA and mutant DNAJB8 canceling experiments, and DNAJB8 is thus an HSP40 family member that has oncogenic potential. CSCs/CICs are known to be resistant to several stresses, including chemotherapy and radiotherapy (15), and overexpression of DNAJB8 might be related to the antistress ability and resistance to treatments.

We observed that overexpression of DNAJB8 increased the percentage of SP cells; however, we still detected MP cells in ACHN/DNAJB8 cells. With regard to tumor-initiating ability, ACHN/DNAJB8 SP cells showed higher tumor-initiating ability than that of ACHN/DNAJB8 MP cells (Table 1). Because both ACHN/DNAJB8 SP cells and ACHN/DNAJB8 MP cells expressed DNAJB8 at almost same levels (data not shown), these observations suggest the existence of other cofactor for induction of CSCs/CICs. In a previous study, DNAJB8 was shown to have role in inhibition of cytotoxic protein aggregation (22), and it is important for association with HDACs through the C-terminal serine-rich region. We also found that the serine-rich region of DNAJB8 has a role in maintenance of CSCs/CICs. These observations suggest that association with HDACs (HDAC4, HDAC6, and SIRT2) might be important for DNAJB8 functions in CSCs/CICs, and that HDACs are possible candidates of cofactors of DNAJB8.

In this study, we showed for the first time that DNAJB8 can be a target of immunotherapy. Mutated and wild-type HSP70 proteins have been reported to be targets of CTLs (41–43), whereas other HSP family proteins have never been reported to be targets of immunocytes. HSP family proteins are often expressed in several kinds of normal organs, and immunocytes might be immunologically tolerated to those proteins. On the other hand, DNAJB8 is expressed only in the testis, and it is thus a novel CT antigen that is regarded as an ideal immunologic target.

HSP family proteins work as molecular chaperones and bind to their client proteins. Antigenic peptide-bound HSP 70 and 90 family proteins are known to work as immune modulators that enhance the cross-priming pathway and enhance antitumor immunity (44–47). In this study, we confirmed anti-DNAJB8

Nishizawa et al.

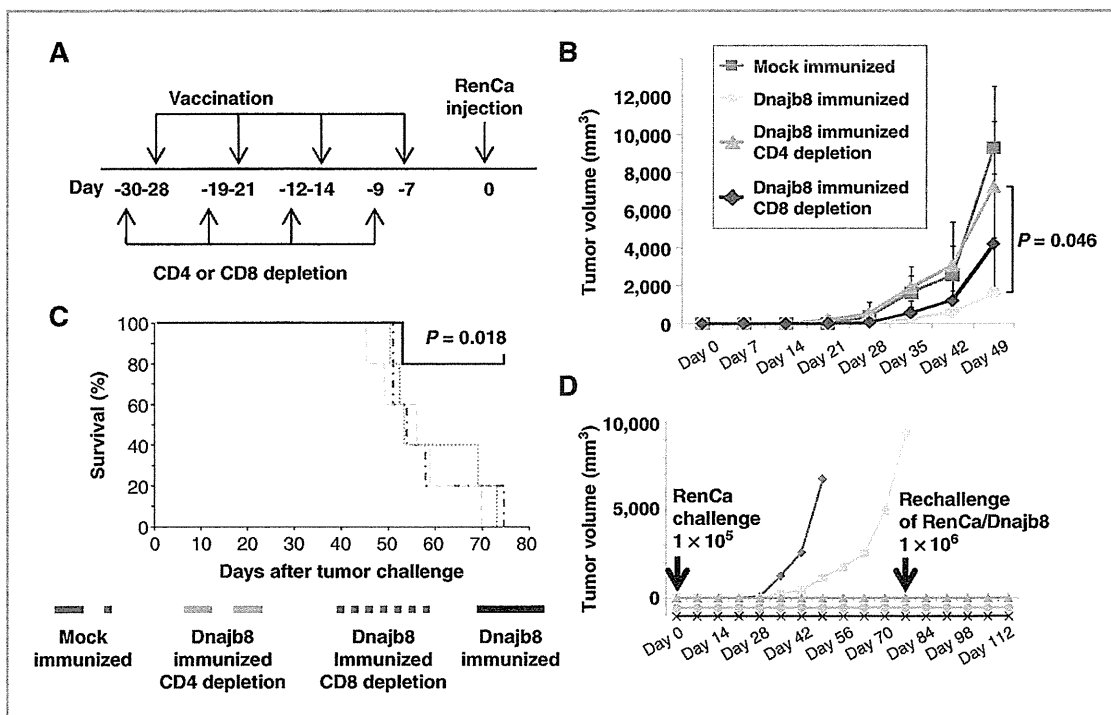


Figure 5. Immunogenicity of DNAJB8. **A**, time course of CD4⁺ or CD8⁺ T cell depletion. CD4⁺ or CD8⁺ cells were depleted 2 days before DNA vaccination by injecting anti-CD4 or anti-CD8 mAb into the peritoneal cavity. **B**, antitumor effects with CD4 or CD8 T-cell depletion. Tumor growth curves of the Mock-immunized group, Dnajb8-immunized group, Dnajb8-immunized CD4-depleted group, and Dnajb8-immunized CD8-depleted group are shown. Data are means \pm SD. **C**, survival curve with CD4 or CD8 T-cell depletion. Mouse survival curves of Mock-immunized group, Dnajb8-immunized group, Dnajb8-immunized CD4-depleted group, and Dnajb8-immunized CD8-depleted group are shown. **D**, rechallenge test with RenCa/DNAJB8 cells. Tumor growth curves of individual mice in the Dnajb8-immunized group are shown. Each curve represents tumor growth in each mouse. Three of 5 mice immunized with Dnajb8 did not show initiation of tumor formation with injection of 1×10^5 RenCa cells at day 70. Thereafter, the 3 mice were rechallenged with 10 times larger numbers of RenCa/DNAJB8 cells (1×10^6) at day 77 and were observed.

immunity with DNAJB8-immunized mouse spleen cells. However, there remains the possibility that DNAJB8 also binds to another antigen protein/peptide and induces antigen-specific immunity, and further investigation should be carried out.

A DNA vaccination experiment revealed that targeting CSC antigen (Dnajb8) was more effective than targeting a shared antigen (Survivin). In a previous study, we found that colon CSCs/CICs can be recognized by an established CTL clone at the same level as non-CSCs/CICs both *in vitro* and *in vivo* (16). We therefore suggest that CTLs are promising tools to target CSCs/CICs. Expression of TAAs is essential for CTL recognition, and we categorized TAAs into 3 groups (CSC antigens, shared antigens, and non-CSC antigens; ref. 17). In a recent study, we found that TAA expression in the CSC/CIC population is necessary to achieve an antitumor effect and that the antitumor effect of a shared antigen is greater than that of non-CSC antigens (48). Then, which is the best target, CSC antigens or shared antigens? In this study, we showed for the first time that a CSC antigen is more effective than a shared antigen. Our results indicate that a CSC antigen has the greatest antitumor effect and a non-CSC antigen has the smallest antitumor effect and that evaluation of the distribution in CSCs/CICs and non-

CSCs/CICs is important to predict the efficiency of antitumor effects of novel TAAs.

We showed that targeting CSCs/CICs is an effective approach for cancer immunotherapy. On the other hand, glioma-associated CSCs/CICs have been reported to be related to immunosuppression through B7-H1 and soluble Galectin-3 and STAT3 signaling (49, 50). These observations suggest that CSCs/CICs might suppress the CTL induction phase but might not affect the CTL effector phase. In this study, we observed a significant antitumor effect with immunization using *Dnajb8*-coding plasmid. This is a prophylactic model and CTL induction might not be affected by CSCs/CICs included in RenCa cells and thus bring about preferable results. Therefore, immunotherapy targeting CSCs/CICs might be useful for suppression of posttreatment tumor recurrence and/or adoptive transfer of established CTLs.

In summary, we identified an HSP40 family protein, DNAJB8, as one of the CT antigens and also as a CSC antigen. DNAJB8 has a role in maintenance of RCC CSCs/CICs. Targeting a CSC antigen is more effective than targeting a shared antigen, and DNAJB8 is a possible candidate for CSC/CIC-targeting immunotherapy.

Disclosure of Potential Conflicts of Interest

No potential conflicts of interest were disclosed.

Authors' Contributions

Conception and design: Y. Hirohashi, T. Torigoe

Development of methodology: Y. Hirohashi, T. Torigoe, A. Takahashi, K. Kamiguchi, A. Sokolovskaya, R. Fujii

Acquisition of data (provided animals, acquired and managed patients, provided facilities, etc.): S. Nishizawa, Y. Hirohashi, T. Torigoe, A. Takahashi, Y. Tamura, H. Asanuma, R. Morita, A. Sokolovskaya, J. Matsuzaki, R. Yamada

Analysis and interpretation of data (e.g., statistical analysis, biostatistics, computational analysis): S. Nishizawa, Y. Hirohashi, T. Torigoe, A. Takahashi, Y. Tamura, H. Asanuma

Writing, review, and/or revision of the manuscript: S. Nishizawa, Y. Hirohashi, T. Torigoe, T. Kanaseki, R. Fujii

Administrative, technical, or material support (i.e., reporting or organizing data, constructing databases): Y. Hirohashi, T. Torigoe, T. Mori, H.H. Kampinga, T. Kondo, I. Hara

Study supervision: Y. Hirohashi, T. Torigoe, T. Hasegawa, N. Sato

Acknowledgments

The authors thank Ms. Eniri Nakazawa and Ms. Eri Saka for technical assistance; Drs K. Inai, K. Itoh, and P.G. Coulie for kindly providing cell lines; and Dr. T. Kitamura for kindly providing a retrovirus system.

Grant Support

This study was supported by a grant-in-aid for Scientific Research from the Ministry of Education, Culture, Sports, Science and Technology of Japan (to N. Sato), program for developing the supporting system for upgrading education and research from the Ministry of Education, Culture, Sports, Science and Technology of Japan (to N. Sato) and Takeda Science Foundation (to Y. Hirohashi).

The costs of publication of this article were defrayed in part by the payment of page charges. This article must therefore be hereby marked *advertisement* in accordance with 18 U.S.C. Section 1734 solely to indicate this fact.

Received September 15, 2011; revised March 12, 2012; accepted March 25, 2012; published OnlineFirst May 2, 2012.

References

- Motzer RJ, Hutson TE, Tomczak P, Michaelson MD, Bukowski RM, Rixe O, et al. Sunitinib versus interferon alfa in metastatic renal-cell carcinoma. *N Engl J Med* 2007;356:115–24.
- Escudier B, Eisen T, Stadler WM, Szczylik C, Oudard S, Siebels M, et al. Sorafenib in advanced clear-cell renal-cell carcinoma. *N Engl J Med* 2007;356:125–34.
- Motzer RJ, Escudier B, Oudard S, Hutson TE, Porta C, Bracarda S, et al. Efficacy of everolimus in advanced renal cell carcinoma: a double-blind, randomised, placebo-controlled phase III trial. *Lancet* 2008;372:449–56.
- Clark JI, Atkins MB, Urba WJ, Creech S, Figlin RA, Dutcher JP, et al. Adjuvant high-dose bolus interleukin-2 for patients with high-risk renal cell carcinoma: a cytokine working group randomized trial. *J Clin Oncol* 2003;21:3133–40.
- Messing EM, Manola J, Wilding G, Prokert K, Fleischmann J, Crawford ED, et al. Phase III study of interferon alfa-NL as adjuvant treatment for resectable renal cell carcinoma: an Eastern Cooperative Oncology Group/Intergroup trial. *J Clin Oncol* 2003;21:1214–22.
- Negrier S, Escudier B, Lasset C, Douillard JY, Savary J, Chevreau C, et al. Recombinant human interleukin-2, recombinant human interferon alfa-2a, or both in metastatic renal-cell carcinoma. *Groupe Français d'Immunothérapie. N Engl J Med* 1998;338:1272–8.
- Hirohashi Y, Torigoe T, Inoda S, Kobayashi J, Nakatsugawa M, Mori T, et al. The functioning antigens: beyond just as the immunological targets. *Cancer Sci* 2009;100:798–806.
- Sato N, Hirohashi Y, Tsukahara T, Kikuchi T, Sahara H, Kamiguchi K, et al. Molecular pathological approaches to human tumor immunology. *Pathol Int* 2009;59:205–17.
- Marchand M, van Baren N, Weynants P, Richard V, Dréno B, Tessier MH, et al. Tumor regressions observed in patients with metastatic melanoma treated with an antigenic peptide encoded by gene MAGE-3 and presented by HLA-A1. *Int J Cancer* 1999;80:219–30.
- Rosenberg SA, Yang JC, Schwartztruber DJ, Hwu P, Marincola FM, Topalian SL, et al. Immunologic and therapeutic evaluation of a synthetic peptide vaccine for the treatment of patients with metastatic melanoma. *Nat Med* 1998;4:321–7.
- Laird AK. Cell fractionation of normal and malignant tissues. *Exp Cell Res* 1954;6:30–44.
- Reya T, Morrison SJ, Clarke MF, Weissman IL. Stem cells, cancer, and cancer stem cells. *Nature* 2001;414:105–11.
- Clarke MF, Dick JE, Dirks PB, Eaves CJ, Jamieson CH, Jones DL, et al. Cancer stem cells—perspectives on current status and future directions: AACR Workshop on cancer stem cells. *Cancer Res* 2006;66:9339–44.
- Hirohashi Y, Torigoe T, Inoda S, Takahashi A, Morita R, Nishizawa S, et al. Immune response against tumor antigens expressed on human cancer stem-like cells/tumor-initiating cells. *Immunotherapy* 2010;2: 201–11.
- Park CY, Tseng D, Weissman IL. Cancer stem cell-directed therapies: recent data from the laboratory and clinic. *Mol Ther* 2009;17:219–30.
- Inoda S, Hirohashi Y, Torigoe T, Morita R, Takahashi A, Asanuma H, et al. Cytotoxic T lymphocytes efficiently recognize human colon cancer stem-like cells. *Am J Pathol* 2011;178:1805–13.
- Hirohashi Y, Torigoe T, Inoda S, Morita R, Kochin V, Sato N. Cytotoxic T lymphocytes: Sniping cancer stem cells. *Oncimmunology* 2012;1: 123–5.
- Nakatsugawa M, Hirohashi Y, Torigoe T, Asanuma H, Takahashi A, Inoda S, et al. Novel spliced form of a lens protein as a novel lung cancer antigen, Lengsin splicing variant 4. *Cancer Sci* 2009;100: 1485–93.
- Inoda S, Hirohashi Y, Torigoe T, Nakatsugawa M, Kiriya K, Nakazawa E, et al. Cep55/c10orf3, a tumor antigen derived from a centrosome residing protein in breast carcinoma. *J Immunother* 2009;32: 474–85.
- Goodell MA, Brose K, Paradis G, Conner AS, Mulligan RC. Isolation and functional properties of murine hematopoietic stem cells that are replicating in vivo. *J Exp Med* 1996;183:1797–806.
- Morita S, Kojima T, Kitamura T. Plat-E: an efficient and stable system for transient packaging of retroviruses. *Gene Ther* 2000;7:1063–6.
- Hageman J, Rujano MA, van Waarde MA, Kakkar V, Dirks RP, Govorkhina N, et al. A DNAJB chaperone subfamily with HDAC-dependent activities suppresses toxic protein aggregation. *Mol Cell* 2010;37: 355–69.
- Boon T, Cerottini JC, Van den Eynde B, van der Bruggen P, Van Pel A. Tumor antigens recognized by T lymphocytes. *Annu Rev Immunol* 1994;12:337–65.
- Burkert J, Otto WR, Wright NA. Side populations of gastrointestinal cancers are not enriched in stem cells. *J Pathol* 2008;214:564–73.
- Mani SA, Guo W, Liao MJ, Eaton EN, Ayyanan A, Zhou AY, et al. The epithelial-mesenchymal transition generates cells with properties of stem cells. *Cell* 2008;133:704–15.
- Hirohashi Y, Torigoe T, Maeda A, Nabeta Y, Kamiguchi K, Sato T, et al. An HLA-A24-restricted cytotoxic T lymphocyte epitope of a tumor-associated protein, survivin. *Clin Cancer Res* 2002;8:1731–9.
- Siegel S, Wagner A, Schmitz N, Zeis M. Induction of antitumor immunity using survivin peptide-pulsed dendritic cells in a murine lymphoma model. *Br J Haematol* 2003;122:911–4.
- Andersen MH, Svane IM, Becker JC, Straten PT. The universal character of the tumor-associated antigen survivin. *Clin Cancer Res* 2007;13:5991–4.
- Hofmann UB, Voigt H, Andersen MH, Straten PT, Becker JC, Eggert AO. Identification and characterization of survivin-derived H-2Kb-restricted CTL epitopes. *Eur J Immunol* 2009;39:1419–24.
- Berruti G, Perego L, Borgonovo B, Martegani E. MSJ-1, a new member of the DNAJ family of proteins, is a male germ cell-specific gene product. *Exp Cell Res* 1998;239:430–41.

31. Doiguchi M, Kaneko T, Urasoko A, Nishitani H, Iida H. Identification of a heat-shock protein Hsp40, DjB1, as an acrosome- and a tail-associated component in rodent spermatozoa. *Mol Reprod Dev* 2007;74:223-32.
32. Guan J, Yuan L. A heat-shock protein 40, DNAJB13, is an axoneme-associated component in mouse spermatozoa. *Mol Reprod Dev* 2008;75:1379-86.
33. Terada K, Yomogida K, Imai T, Kiyonari H, Takeda N, Kadomatsu T, et al. A type I DnaJ homolog, DJA1, regulates androgen receptor signaling and spermatogenesis. *EMBO J* 2005;24:611-22.
34. Kondo T, Setoguchi T, Taga T. Persistence of a small subpopulation of cancer stem-like cells in the C6 glioma cell line. *Proc Natl Acad Sci U S A* 2004;101:781-6.
35. Murase M, Kano M, Tsukahara T, Takahashi A, Torigoe T, Kawaguchi S, et al. Side population cells have the characteristics of cancer stem-like cells/cancer-initiating cells in bone sarcomas. *Br J Cancer* 2009;101:1425-32.
36. Nakatsugawa M, Takahashi A, Hirohashi Y, Torigoe T, Inoda S, Murase M, et al. SOX2 is overexpressed in stem-like cells of human lung adenocarcinoma and augments the tumorigenicity. *Lab Invest* 2011;91:1796-804.
37. Addla SK, Brown MD, Hart CA, Ramani VA, Clarke NW. Characterization of the Hoechst 33342 side population from normal and malignant human renal epithelial cells. *Am J Physiol Renal Physiol* 2008;295:F680-7.
38. Oates JE, Grey BR, Addla SK, Samuel JD, Hart CA, Ramani VA, et al. Hoechst 33342 side population identification is a conserved and unified mechanism in urological cancers. *Stem Cells Dev* 2009;18:1515-22.
39. Whitesell L, Lindquist SL. HSP90 and the chaperoning of cancer. *Nat Rev Cancer* 2005;5:761-72.
40. Mitra A, Shevde LA, Samant RS. Multi-faceted role of HSP40 in cancer. *Clin Exp Metastasis* 2009;26:559-67.
41. Gaudin C, Kremer F, Angevin E, Scott V, Triebel F. A hsp70-2 mutation recognized by CTL on a human renal cell carcinoma. *J Immunol* 1999;162:1730-8.
42. Azuma K, Shichijo S, Takedatsu H, Komatsu N, Sawamizu H, Itoh K. Heat shock cognate protein 70 encodes antigenic epitopes recognized by HLA-B4601-restricted cytotoxic T lymphocytes from cancer patients. *Br J Cancer* 2003;89:1079-85.
43. Faure O, Graff-Dubois S, Bretaudeau L, Derré L, Gross DA, Alves PM, et al. Inducible Hsp70 as target of anticancer immunotherapy: Identification of HLA-A*0201-restricted epitopes. *Int J Cancer* 2004;108:863-70.
44. Kurotaki T, Tamura Y, Ueda G, Oura J, Kutomi G, Hirohashi Y, et al. Efficient cross-presentation by heat shock protein 90-peptide complex-loaded dendritic cells via an endosomal pathway. *J Immunol* 2007;179:1803-13.
45. Kutomi G, Tamura Y, Okuya K, Yamamoto T, Hirohashi Y, Kamiguchi K, et al. Targeting to static endosome is required for efficient cross-presentation of endoplasmic reticulum-resident oxygen-regulated protein 150-peptide complexes. *J Immunol* 2009;183:5861-9.
46. Oura J, Tamura Y, Kamiguchi K, Kutomi G, Sahara H, Torigoe T, et al. Extracellular heat shock protein 90 plays a role in translocating chaperoned antigen from endosome to proteasome for generating antigenic peptide to be cross-presented by dendritic cells. *Int Immunol* 2011;23:223-37.
47. Tamura Y, Hirohashi Y, Kutomi G, Nakanishi K, Kamiguchi K, Torigoe T, et al. Tumor-produced secreted form of binding of immunoglobulin protein elicits antigen-specific tumor immunity. *J Immunol* 2011;186:4325-30.
48. Mori T, Nishizawa S, Hirohashi Y, Torigoe T, Tamura Y, Takahashi A, et al. Efficiency of G2/M-related tumor-associated antigen-targeting cancer immunotherapy depends on antigen expression in the cancer stem-like population. *Exp Mol Pathol* 2012;92:27-32.
49. Wei J, Barr J, Kong LY, Wang Y, Wu A, Sharma AK, et al. Glioblastoma cancer-initiating cells inhibit T-cell proliferation and effector responses by the signal transducers and activators of transcription 3 pathway. *Mol Cancer Ther* 2010;9:67-78.
50. Wei J, Barr J, Kong LY, Wang Y, Wu A, Sharma AK, et al. Glioma-associated cancer-initiating cells induce immunosuppression. *Clin Cancer Res* 2010;16:461-73.

Heat shock enhances the expression of cytotoxic granule proteins and augments the activities of tumor-associated antigen-specific cytotoxic T lymphocytes

Akari Takahashi · Toshihiko Torigoe · Yasuaki Tamura · Takayuki Kanaseki · Tomohide Tsukahara · Yasushi Sasaki · Hidekazu Kameshima · Tetsuhiro Tsuruma · Koichi Hirata · Takashi Tokino · Yoshihiko Hirohashi · Noriyuki Sato

Received: 1 February 2012 / Revised: 19 June 2012 / Accepted: 21 June 2012 / Published online: 11 July 2012
© Cell Stress Society International 2012

Abstract Focal inflammation causes systemic fever. Cancer hyperthermia therapy results in shrinkage of tumors by various mechanisms, including induction of adaptive immune response. However, the physiological meaning of systemic fever and mechanisms of tumor shrinkage by hyperthermia have not been completely understood. In this study, we investigated how heat shock influences the adaptive immune system. We established a cytotoxic T lymphocyte (CTL) clone (#IM29) specific for survivin, one of the tumor-associated antigens (TAAs), from survivin peptide-immunized cancer patients' peripheral blood, and the CTL activities were investigated in several temperature conditions (37–41 °C). Cytotoxicity and IFN- γ secretion of CTL were greatest under 39 °C condition, whereas they were minimum under 41 °C. To address the molecular

mechanisms of this phenomenon, we investigated the apoptosis status of CTLs, expression of CD3, CD8, and TCR $\alpha\beta$ by flow cytometry, and expression of perforin, granzyme B, and Fas ligand by western blot analysis. The expression of perforin and granzyme B were upregulated under temperature conditions of 39 and 41 °C. On the other hand, CTL cell death was induced under 41 °C condition with highest Caspase-3 activity. Therefore, the greatest cytotoxicity activity at 39 °C might depend on upregulation of cytotoxic granule proteins including perforin and granzyme B. These results suggest that heat shock enhances effector phase of the adaptive immune system and promotes eradication of microbe and tumor cells.

Keywords Heat shock · CTL · Perforin · Survivin

Electronic supplementary material The online version of this article (doi:10.1007/s12192-012-0348-0) contains supplementary material, which is available to authorized users.

A. Takahashi · T. Torigoe (✉) · Y. Tamura · T. Kanaseki · T. Tsukahara · Y. Sasaki · Y. Hirohashi (✉) · N. Sato
Department of Pathology,
Sapporo Medical University School of Medicine,
South-1 West-17, Chuo-Ku,
Sapporo 060-8556, Japan
e-mail: torigoe@sapmed.ac.jp
e-mail: hirohash@sapmed.ac.jp

Y. Sasaki · T. Tokino
Department of Medical Genome Sciences,
Research Institute for Frontier Medicine,
Sapporo Medical University School of Medicine,
South-1 West-17, Chuo-Ku,
Sapporo 060-8556, Japan

H. Kameshima · T. Tsuruma · K. Hirata
Department of Surgery,
Sapporo Medical University School of Medicine,
South-1 West-17, Chuo-Ku,
Sapporo 060-8556, Japan

Abbreviations

CTL	Cytotoxic T lymphocyte
TAA	Tumor-associated antigen
HLA	Human leukocyte antigen
PBMC	Peripheral blood mononuclear cell
mAb	Monoclonal antibody
HSP	Heat shock protein

Introduction

Inflammation is defined by four classical signs, pain (dolor), heat (calor), redness (rubor), and swelling (tumor), caused by secretion of inflammatory cytokines (e.g., IL-1 β , TNF α , and IL-6) from inflammatory cells (Bernheim et al. 1979). Inflammatory cytokines induce the secretion of prostaglandin E2 from endothelial cells of the central nervous system, and prostaglandin E2 acts in the hypothalamic area, resulting in fever. Although fever is one of the well-described symptoms of

Table 1 Summary of antibodies

Antigen	Company	Clone	Dilution	Application
CD3	Beckman Coletr	UCHT1		Flow cytometry
CD8	BD	SK1		Flow cytometry
TCR $\alpha\beta$	Thermo scientific	BMA031		Flow cytometry
HLA-A24	- ^a	C7709A2.6	Culture sup.	Flow cytometry
Fas Ligand	MBL	CH-11	1000	Western blot
Perforin	SIGMA	3B4	1000	Western blot
Granzyme B	R&D systems	351927	1000	Western blot
HSP90	Enzo Life Sciences	AC88	1000	Western blot
HSP70	Enzo Life Sciences		1000	Western blot
Fas Ligand	R&D systems	#154922	1000	Western blot
β -actin	SIGMA	AC15	2000	Western blot

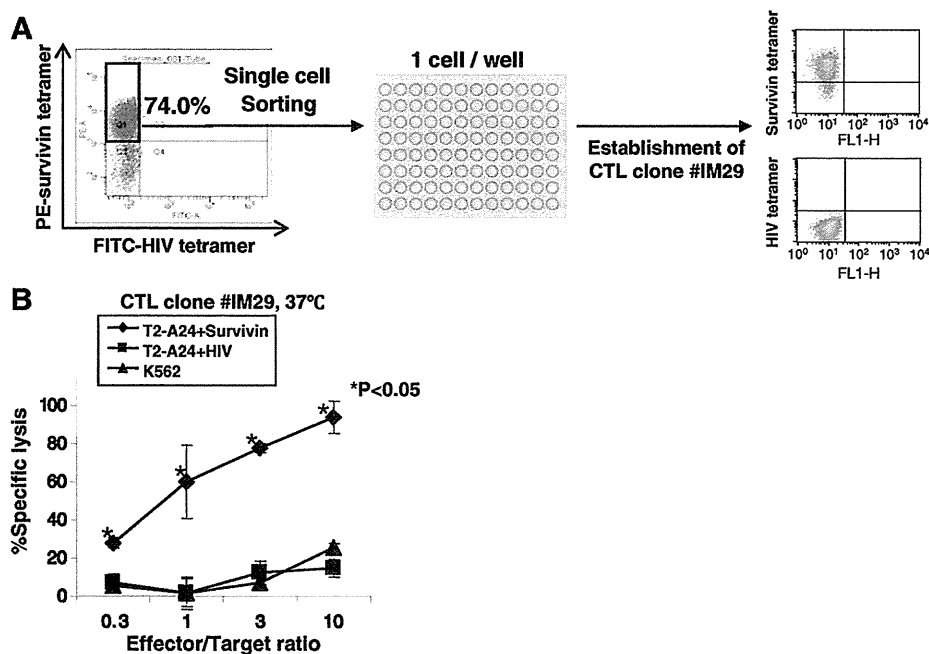
^aKind gift from Dr. P. G. Coulie

inflammation, the physiological meanings on adaptive immunity involving cytotoxic T lymphocytes (CTLs) still remain unclear.

Hyperthermia for cancer treatment has been of clinical interest for many years, though the exact anti-tumor mechanism remains unclear. Several reports have indicated that heat treatment enhanced adaptive immune response by CTL cross-priming due to induction of heat shock proteins (HSPs). HSPs associated with antigenic peptides and HSPs induced by heat treatment in cancer cells enhance cancer-specific adaptive immune responses by cross-priming (Bachleitner-Hofmann et al. 2006; Brusa et al. 2009; Sato et al. 2009, 2010; Shi et al. 2006; Torigoe et al. 2009). On the other hand, the direct effects of heat treatment on established CTLs remain unknown.

In this study, we investigated the effect of heat treatment on a CTL clone specific for survivin, one of the tumor-associated antigens (TAAs; Hirohashi et al. 2002). Heat treatment (39 °C) of CTLs enhanced the cytotoxicity and the secretion of IFN- γ of CTLs, whereas heat treatment with higher temperature (41 °C) abrogated CTL functions. To address the molecular mechanism of this phenomenon, we examined changes in the expression of several molecules in CTLs and found that the expression of cytotoxic granule proteins (perforin and granzyme B) is enhanced by heat treatment. On the other hand, the expression of CD3, CD8, and TCR B did not show any difference. The viability of CTLs was abrogated and apoptotic cells were increased by higher heat treatment (41 °C). These findings indicate that heat treatment of CTLs at 39 °C enhances CTL functions

Fig. 1 Establishment of CTL clone #IM29. **a** Schematic summary of establishment of CTL clone. Survivin tetramer-positive cells were single-cell-sorted into a 96-well plate at single cell per well. The specificity of growing T cells was assessed by survivin- and HIV-tetramer staining. **b** Cytotoxicity of CTL clone #IM29. Cytotoxicity of CTL clone #IM29 was evaluated with survivin peptide-pulsed T2-A24 cells, control peptide (HIV)-pulsed T2-A24 cells and K562 cells. Asterisks represent significant difference compared with HIV peptide-pulsed T2-A24 cells or K562 cells ($P < 0.05$, t test). Data are mean \pm SD



partially by upregulation of perforin and granzyme B, and that heat treatment of CTLs at 41 °C abrogates CTL functions partially by inducing apoptosis. Augmentation of CTL functions by heat treatment might be one significant reason of fever induced by inflammation and also one mechanism of hyperthermia.

Materials and methods

Cells and antibodies

T2-A24 cells, human leukocyte antigen (HLA)-A24 gene-transduced T2 cells, were a kind gift from Dr. K. Kuzushima (Nagoya, Japan). The cells were cultured in RPMI1640 (SIGMA) supplemented with 10 % FBS (Life Technologies) and 800 µg/ml of G418 (Life Technologies). K562 cells were obtained from ATCC and

cultured in RPMI1640 supplemented with 10 % FBS. The antibodies used in this study are summarized in Table 1.

Establishment of CTL clone #IM29

A survivin peptide-specific CTL clone was established from peripheral blood of a 44-year-old patient with rectal carcinoma who was treated with survivin peptide immunization and IFN α (Kameshima et al. 2011). Survivin peptide-specific CTLs were stained with survivin peptide-HLA-A24 complex tetramer and were single-cell-sorted by FACS Aria II (BD) into a round-bottomed 96-well plate at single cell per well. The CTL was incubated with irradiated 8×10^4 peripheral blood mononuclear cells (PBMCs) in AIM-V (Life Technologies) medium supplemented with 10 % human AB serum (kindly provided by Dr. Tatsuo Usui, Hokkaido Red

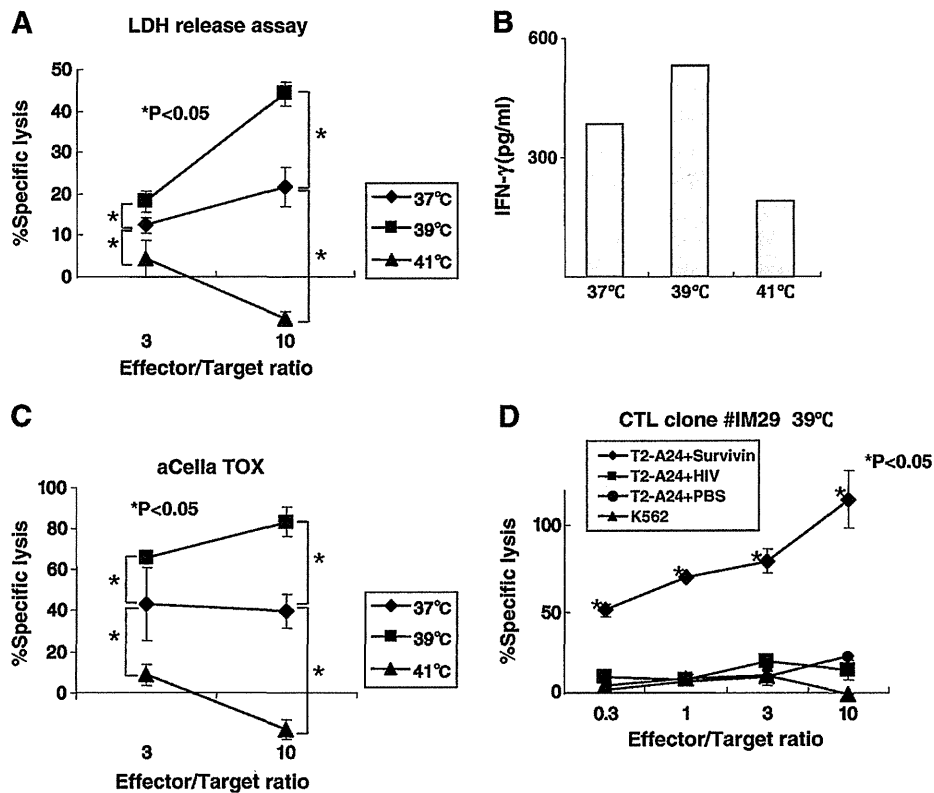


Fig. 2 Heat treatment enhances CTL functions. **a** Cytotoxicity of CTL clone #IM29 in several temperature conditions. Cytotoxicity of CTL clone #IM29 using T2-A24 cells pulsed with survivin peptide was evaluated by LDH release assay under several temperature conditions (37, 39, and 41 °C). Asterisks represent significant difference ($P < 0.05$, t test). Data are mean \pm SD. **b** IFN- γ secretion of CTL clone #IM29 in several temperature conditions. IFN- γ secretion of CTL clone #IM29 using T2-A24 cells pulsed with survivin peptide was evaluated by ELISA under several temperature conditions (37, 39, and 41 °C). Data are mean. **c** Cytotoxicity of CTL clone #IM29 using aCella TOX assay.

Cytotoxicity of CTL clone #IM29 using T2-A24 cells pulsed with survivin peptide was evaluated by aCella TOX assay under several temperature conditions (37, 39, and 41 °C). Asterisks represent significant difference ($P < 0.05$, t test). Data are mean \pm SD. **d** Cytotoxicity of CTL clone #IM29 in 39 °C condition. CTLs were preincubated in 39 °C for 1 day before cytotoxicity assay. Cytotoxicity of CTL clone #IM29 was evaluated with survivin peptide-pulsed T2-A24 cells, control peptide (HIV)-pulsed T2-A24 cells and K562 cells in 39 °C. Asterisks represent significant difference compared with HIV peptide-pulsed T2-A24 cells or K562 cells ($P < 0.05$, t test). Data are mean \pm SD.

Cross Blood Center, Sapporo, Japan), 200 IU of IL-2 (R&D Systems), and 5 $\mu\text{g}/\text{ml}$ of PHA (SIGMA). Growing wells were transferred into a 24-well plate and fed every 3 days with AIM-V supplemented with 10 % human AB serum and 200 IU of IL-2. On day 34, clones were assessed by survivin tetramer staining and HIV-tetramer as a negative control (Fig. 1a). Tetramers were obtained from MBL Co., Ltd. (Nagoya, Japan).

Cytotoxicity assay and IFN- γ ELISA

CTL clone #IM29 were preincubated at 37–41 °C for 1 day before cytotoxicity assay and IFN- γ ELISA. Survivin peptide-pulsed T2-A24 cells were seeded into a 96-well plate at 5×10^3 cells/well. CTL clone #IM29 cells were seeded at several effector/target (*E/T*) ratios, then incubated at 37–41 °C for 6 h. Cytotoxicity of CTL clone #IM29 cells was examined by using an LDH cytotoxicity detection kit (TAKARA BIO Inc., Osaka, Japan) and aCella TOX kit (Cell Technology, Inc., Mountain View, CA) according to the manufacturer's protocol.

Ten thousand survivin peptide-pulsed T2-A24 cells and 3×10^3 of CTL clone #29 cells were co-cultured in a 96-well plate at 37–41 °C for 12 h, and then IFN- γ concentrations in supernatants were measured by using a Human IFN gamma ELISA Kit (Thermo Scientific) as described in the manufacturer's protocol.

Live images of cytotoxicity were recorded by the OLYMPUS FLUOVIEW FV 300-I71BG-SP system (OLYMPUS). Briefly, T2-A24 cells were transduced with GFP-plasmid using a Nucleofector V kit (Amaxa). GFP-positive T2-A24 cells were pulsed with survivin peptide and co-cultured with CTL clone #IM29 cells at an *E/T* ratio=10, and cultured in 37–41 °C for 4 h and live image were recorded.

Flow cytometry

For detection of HLA-A24 of T2-A24 cells, T2-A24 cells were stained with anti-HLA-A24 mAb (C7709A2.6, kind gift from Dr. P. G. Coulie, Brussels, Belgium) for 1 h, washed three times with PBS, stained with FITC-labeled anti-mouse IgG+M antibody (KPL, 200 times dilution) for 30 min, and washed again one time with PBS. T2-A24 cells were analyzed by a FACS Calibur (BD).

After treatment of CTL clone #IM29 cells at 37–41 °C for 12 h, the expression of CD3, CD8, and TCR $\alpha\beta$ was examined by ad FACS Calibur. After staining with first antibodies (summarized in Table 1), CTL clone #IM29 cells were stained with FITC-labeled anti-mouse IgG+M antibody and then analyzed by a FACS Calibur. Mean fluorescent intensity was calculated by CELL Quest software (BD).

Western blot

Western blot analysis was performed as described previously (Nakatsugawa et al. 2011). Anti-perforin, granzyme B, Fas ligand, HSP90, and β -actin mAbs were used at 1,000 \times , 1,000 \times , 1,000 \times , 1,000 \times , and 2,000 \times dilutions, respectively (summarized in Table 1). The specific bands were quantified by using Image J software (NIH).

Detection of apoptosis

Apoptotic cells were detected by staining with anti-annexin V antibody and propidium iodide (PI) using annexin V FLUOD staining kit (Roche) according to the manufacturer's protocol and then analyzed by a FACS Calibur. For detection of dead cells, CTLs were stained with Trypan Blue (Life Technologies) and % dead cells were calculated by Countess Automated Cell Counter (Life Technologies). Caspase-3 activity was measured by using APOPCYTO Caspase-3 Colorimetric Assay Kit (MBL, Nagoya, Japan) according to the manufacturer's protocol. CTLs were preincubated under 37–41 °C conditions for 24 h, before caspase-3 assay.

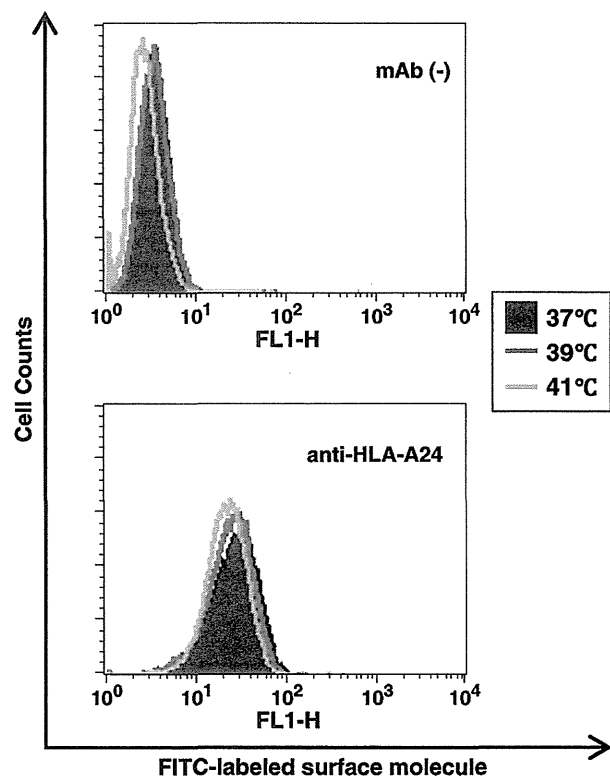


Fig. 3 Heat shock did not alter HLA-A24 expression on T2-A24 cells. The expression of HLA-A24 on T2-A24 cells under several temperature conditions was evaluated by a FACS Calibur. Mean fluorescent intensity (MFI) are listed in ESM 5

Results

Establishment of survivin-derived antigenic peptide-specific CTL clone

To establish a CTL clone specific for cancer cells, we sorted survivin peptide-specific CTLs using survivin peptide-

HLA-A24 complex tetramer (Fig. 1a). Sorted CTLs were grown in 96-well plates and a survivin tetramer-positive CTL clone (#IM29) was established (Fig. 1a). CTL clone #IM29 recognized survivin peptide-pulsed T2-A24 cells at different *E/T* ratios, whereas it did not recognize control peptide-pulsed T2-A24 cells or K562 cells, indicating that CTL clone #IM29 is specific for survivin peptide (Fig. 1b).

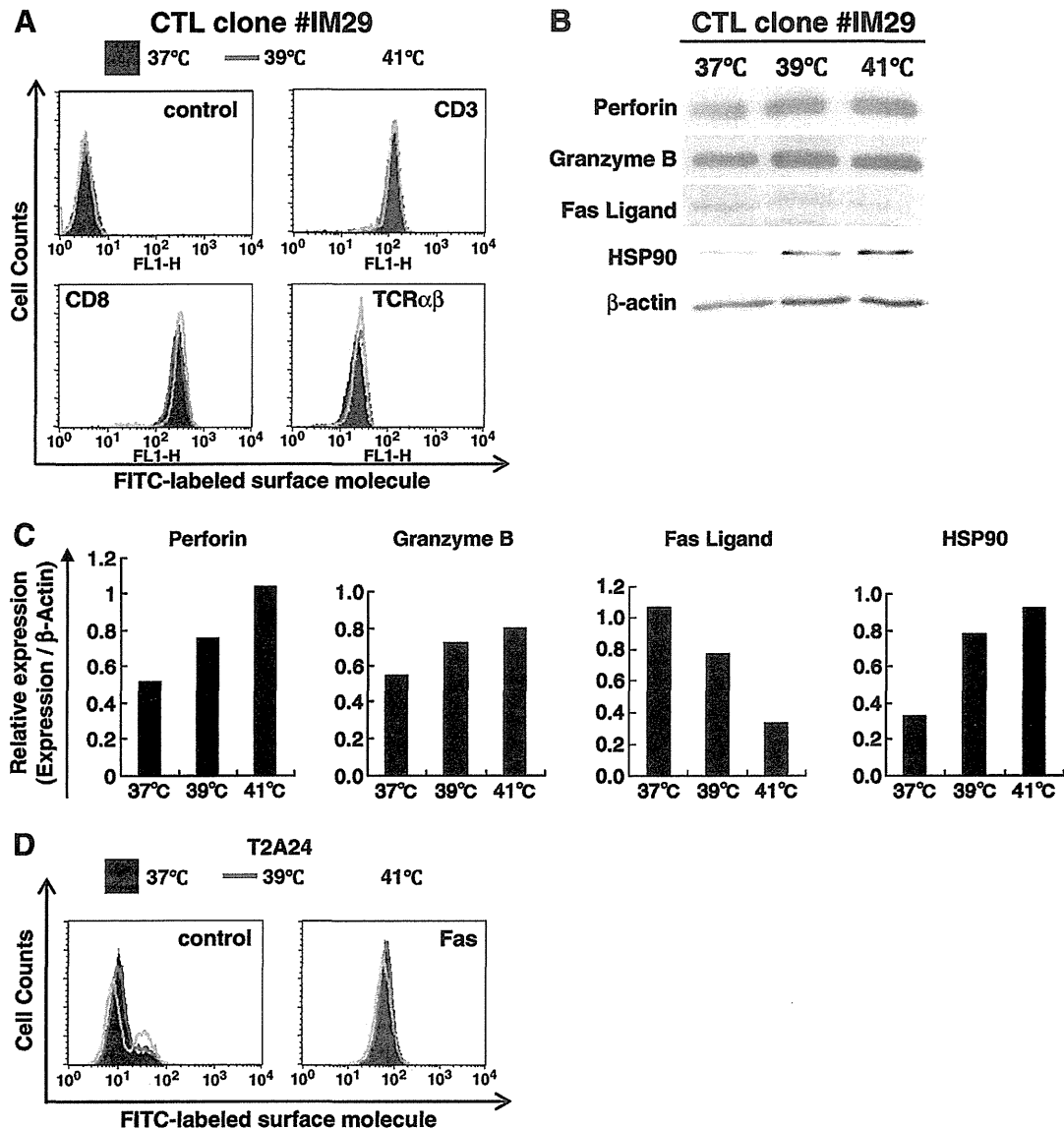


Fig. 4 Expression of several molecules of CTL in several temperature conditions. **a** Flow cytometer analysis of surface molecules on CTL clone #IM29 cells under several temperature conditions. CD3, CD8 and TCR $\alpha\beta$ expression on CTL clone #IM29 under several temperature conditions was analyzed by using a flow cytometer. Mean fluorescent intensity (MFI) are listed in ESM 6. **b** Western blot analysis of CTL clone #IM29 under several temperature conditions. Perforin, granzyme B, Fas ligand and HSP90 protein expression in CTL clone #IM29 under several temperature conditions was analyzed by western blot analysis. β -Actin was used as a

internal positive control. Data are representative Western Blot pictures. **c** Quantification of protein expression in CTL clone #IM29 under several temperature conditions. Western blot bands were analyzed, and quantified by Image J software (NIH). Perforin, granzyme B, Fas ligand, and HSP90 expression were standardized by β -Actin. Data are relative expression of perforin, granzyme B, Fas ligand and HSP90. **d** Heat shock did not alter Fas expression on T2-A24 cells. The expression of Fas on T2-A24 cells under several temperature conditions was evaluated by a FACS Calibur. Mean fluorescent intensity (MFI) are listed in ESM 7

Heat treatment enhanced CTL functions

To address the effects of heat treatment on CTL functions, we evaluated CTL functions under several temperature (37–41 °C) conditions (Fig. 2a, b, c and Electronic supplementary material (ESM)). Cytotoxicity of CTL was significantly enhanced in 39 °C condition compared with 37 °C condition, whereas the cytotoxicity was decreased in 41 °C condition by LDH release assay (Fig. 2a). IFN- γ secretion also showed similar pattern as cytotoxicity with highest IFN- γ secretion in 39 °C condition (Fig. 2b). To confirm the cytotoxicity results using LDH release assay, we performed aCella TOX assay. aCella TOX assay also showed that the cytotoxicity of CTL was greatest in 39 °C condition, and minimum in 41 °C (Fig. 2c). The specificity of CTL was not altered in 39 °C condition indicating that heat shock enhances only antigenic peptide-specific cytotoxicity, but not non-specific cytotoxicity (Fig. 2d).

Heat shock induced the HSP70 expression in T2-A24 cells (Supplemental data 4), whereas the expression of HLA-A24 molecule on T2-A24 cells was not enhanced under heat shock conditions (Fig. 3).

Heat treatment upregulated the expression of perforin

CTLs recognize target cells through cell surface molecules, including CD3, CD8, and TCR $\alpha\beta$, and kill target cells by secretion of cytotoxic granule proteins including perforin and granzyme B. We investigated the expression of these molecules in CTLs under several temperature conditions (Fig. 4a and b). The expression of CD3, CD8, and TCR $\alpha\beta$ on the surface of CTLs were almost the same in all temperature conditions (37–41 °C; Fig. 4a and b). On the other hand, the expression of perforin and granzyme B were enhanced in high temperature conditions (39 °C and 41 °C) compared with its expression in 37 °C condition (Fig. 4b and c). Fas ligand protein, another cytotoxic molecule expression and Fas expression on T2-A24 cells did not show any increase (Fig. 4b and d).

Heat treatment (41 °C) increased apoptotic cell death of CTLs

Since CTL activity was minimum in the condition of 41 °C, we investigated the cell conditions of CTLs in several

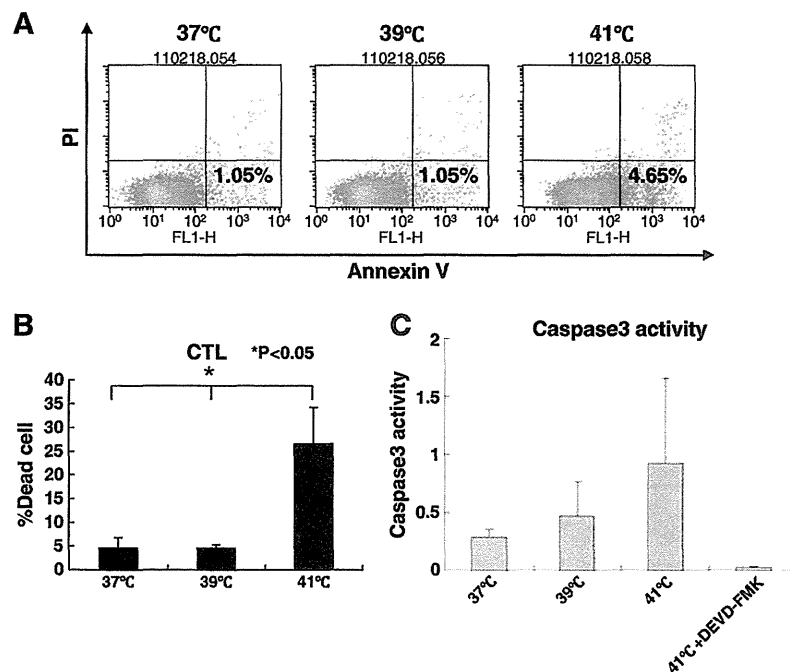


Fig. 5 Apoptotic cell death was induced under 41 °C condition. **a** Detection of apoptosis under several temperature conditions. Apoptotic cell death was detected by anti-annexin V and propidium iodide (PI) staining under several temperature conditions. Percentages represent apoptotic cells (annexin V-positive and PI-negative cells). **b** Percent dead cells was increased in 41 °C. CTLs were preincubated in 37–41 °C

for 1 day. CTLs were stained with Trypan Blue and %dead cells were counted by Countess Automated Cell Counter. Asterisks represent significant difference ($P < 0.05$, t test). Data are mean \pm SD. **c** Caspase 3 was activated in 41 °C. CTLs were preincubated in 37–41 °C for 1 day. Caspase 3 activities were measured by APOPCYTO Caspase-3 Colorimetric Assay Kit. Data are mean \pm SD

temperature conditions. Trypan Blue staining of CTLs cultured in several temperatures revealed that the percentage of dead cells was highest in 41 °C condition (Fig. 5b). To address the type of cell death, annexin V and PI staining was performed to detect apoptotic cell, which were greater at 41 °C than in other temperature conditions (Fig. 5a); and Caspase-3 activity was highest in the 41 °C condition (Fig. 5c). Thus, the CTL cell death partially by apoptosis under 41 °C condition might be the reason of low CTL activity in high temperature.

Discussion

The physiological meaning of fever caused by inflammation has been a major issue for a long time. In this study, we showed for the first time that CTL activity was upregulated by heat treatment. Results of the cytotoxicity assay and IFN- γ assay showed that CTL activity was greatest at 39 °C and that it was the minimum at 41 °C. These observations indicate that fever caused by systemic inflammatory cytokine release enhances CTL functions, and this might enhance eradication of pathogens. The enhancement of cytotoxicity might depend on upregulation of cytotoxic granule proteins including perforin and granzyme B. After secretion from CTLs, perforin is inserted into the plasma membrane, make pore and lyse target cells. Upregulation of cytotoxic granule proteins might not be involved in the enhancement of IFN- γ secretion, suggesting the existence of another molecular mechanism to enhance CTL functions by heat shock.

The exact molecular mechanisms by which cytotoxic granule proteins are upregulated in heat-treated CTLs remain unclear. Since we treated CTLs at 39 °C, it may be transcription enhanced due to the activation of heat shock factor-1 (HSF1); however, there is no HSF1-binding site (heat shock element) in the promoter region of perforin and granzyme B. (Pipkin et al. 2010) Another possible explanation is stabilization of perforin protein by heat treatment. Heat treatment induces upregulation of several chaperone proteins including HSPs by HSF1, and thus association with these chaperone proteins may stabilize and prolong the life span of cytotoxic granule proteins. Further analysis is needed to clarify the exact molecular mechanisms.

Hyperthermia is one treatment modality for cancers, but the exact mechanisms by which it works to suppress cancers remain unclear. Adaptive immune systems induced by antigenic peptides bound to HSPs might be mechanisms (enhancement of induction phase of CTL). In this study, we showed that heat treatment enhanced the cytotoxicity activity of CTLs (enhancement of effector phase of CTL). Therefore, heat treatment will

enhance both induction and effector phases of adaptive immune system. These two mechanisms should act synergistically, and the adaptive immune system should have a role in hyperthermia.

In summary, we showed for the first time that heat treatment of CTLs enhanced CTL functions. Upregulation of cytotoxic granule proteins may play a role in this phenomenon. Enhancement of CTL functions by heat treatment might have a role in CTL functions in fever and hyperthermia.

Acknowledgments The authors thank Ms. E. Nakazawa for technical assistance. The authors thank Dr. Tatsuo Usui (Hokkaido Red Cross Blood Center, Sapporo, Japan) for the kind donation of human sera. The authors thank Dr. K. Kuzushima and Dr. P. G. Coulie for providing cells. This work was supported by Grants-in-Aid for Scientific Research from the Ministry of Education, Culture, Sports, Science and Technology of Japan (grant Nos. 16209013, 17016061 and 15659097) for Practical Application Research from the Japan Science and Technology Agency, and for Cancer Research (15-17 and 19-14) from the Ministry of Health, Labor and Welfare of Japan, Ono Cancer Research Fund (to N. S.) and Takeda Science Foundation (to Y. H.). This work was supported in part by the National Cancer Center Research and Development Fund (23-A-44).

Declaration of financial disclosure The authors have no financial conflict of interest.

References

- Bachleitner-Hofmann T et al (2006) Heat shock treatment of tumor lysate-pulsed dendritic cells enhances their capacity to elicit anti-tumor T cell responses against medullary thyroid carcinoma. *J Clin Endocrinol Metab* 91:4571–4577
- Bernheim HA et al (1979) Fever: pathogenesis, pathophysiology, and purpose. *Ann Intern Med* 91:261–270
- Brusa D et al (2009) Immunogenicity of 56 degrees C and UVC-treated prostate cancer is associated with release of HSP70 and HMGB1 from necrotic cells. *Prostate* 69:1343–1352
- Hirohashi Y et al (2002) An HLA-A24-restricted cytotoxic T lymphocyte epitope of a tumor-associated protein, survivin. *Clin Cancer Res* 8:1731–1739
- Kameshima H et al (2011) Immunogenic enhancement and clinical effect by type-I interferon of anti-apoptotic protein, survivin-derived peptide vaccine, in advanced colorectal cancer patients. *Cancer Sci* 102:1181–1187
- Nakatsugawa M et al (2011) SOX2 is overexpressed in stem-like cells of human lung adenocarcinoma and augments the tumorigenicity. *Lab Invest* 91:1796–1804
- Pipkin ME et al (2010) The transcriptional control of the perforin locus. *Immunol Rev* 235:55–72
- Sato N et al (2009) Molecular pathological approaches to human tumor immunology. *Pathol Int* 59:205–217
- Sato A et al (2010) Melanoma-targeted chemo-thermo-immuno (CTI)-therapy using *N*-propionyl-4-*S*-cysteaminylphenol-magnetite nanoparticles elicits CTL response via heat shock protein-peptide complex release. *Cancer Sci* 101:1939–1946
- Shi H et al (2006) Hyperthermia enhances CTL cross-priming. *J Immunol* 176:2134–2141
- Torigoe T et al (2009) Heat shock proteins and immunity: application of hyperthermia for immunomodulation. *Int J Hyperthermia* 25:610–616

日本臨牀 70 卷 増刊号 8 (2012 年 11 月 20 日発行) 別刷

分子標的薬

—がんから他疾患までの治癒をめざして—

II. 基礎研究

分子標的薬の作用機序・薬理作用

がん関連標的分子・標的経路

熱ショックタンパク質 (heat shock protein: HSP) 系

田村保明

齋藤慶太

佐藤昇志

II 基礎研究

分子標的薬の作用機序・薬理作用
がん関連標的分子・標的経路

熱ショックタンパク質(heat shock protein: HSP)系

Heat shock protein inhibitor for molecular targeting therapy

田村保明 齋藤慶太 佐藤昇志

Key words : 熱ショックタンパク質, Hsp90, 分子シャペロン

はじめに

熱ショックタンパク質(heat shock protein: HSP)は、高温条件などのストレスによって発現が誘導されるタンパク質群で、タンパク質のフォールディングの補助、機能構造の保持、不要タンパク質の凝集や分解などを制御する分子シャペロンとして機能している。なかでも、Hsp90は主要な細胞内分子シャペロンの1つであり、細胞ストレス状況下で発現量が増大するが、定常状態でも細胞内全タンパク質の1-2%を占め、細胞質に最も多く存在するタンパク質の1つである。このHsp90には多くのがん遺伝子産物がクライアントタンパク質として結合しており、それらの機能維持・活性化に重要な役割を果たしている。特に、Hsp90特異的な阻害薬の発見が、最近のHsp90研究の進展に大きく寄与しており、Hsp90の機能の解明に伴いHsp90阻害剤が分子標的薬としてがん治療に貢献するという新しい展望が開けてきた。

1 Hsp90の分子構造

脊椎動物のHsp90には、異なる遺伝子にコードされる2つのアイソフォーム(Hsp90 α , Hsp90 β)が同定されており、そのアミノ酸レベ

ルで約85%の相同性がある。Hsp90は大きく3つのドメインに分かれており、C末端領域を介して恒常的にホモ2量体を形成している(図1)。Hsp90はN末端領域にATP結合ポケットをもつATPaseであり、ATPの加水分解に伴いHsp90自身の2量体構造が大きく変化してオープン型とクローズド型の構造変換のサイクルを繰り返すことで、クライアントタンパク質の結合、フォールディング、機能の維持を行う。通常はC末端ドメインで2量体を形成しオープン型をとるが、ATP結合ポケットにATPが結合するとN末端領域と中間領域との疎水性相互作用が安定化され、中間領域を介してクライアントタンパク質と結合する。更にN末端領域同士が結合してクローズド型Hsp90となる。Hsp90はN末端領域同士が結合した場合にのみATP加水分解活性をもつようになり、N末端領域に結合したATPが加水分解されることによりN末端領域同士の結合が解消されてオープン型となる。

Hsp90阻害剤であるgeldanamycin(GA)やradicicolはHsp90のATP結合ポケットに結合して、オープン型にシフトさせることでクライアントタンパク質の解離を引き起こし、その結果クライアントタンパク質はユビキチン化され、プロテアソームによる分解を受けることにな

Yasuaki Tamura, Keita Saito, Noriyuki Sato: Department of Pathology, Sapporo Medical University School of Medicine 札幌医科大学医学部 病理学第1講座

0047-1852/12/¥60/頁/JCOPY

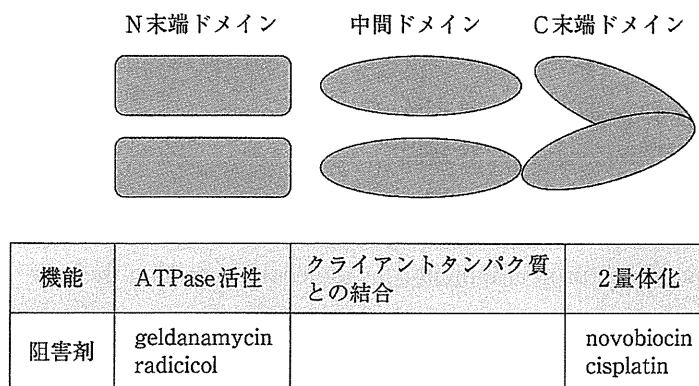


図1 Hsp90の構造と阻害剤作用部位

る^{1,2)}。

2 Hsp90の機能

Hsp90は様々な細胞内タンパク質と相互作用してその正確なフォールディングと機能を保証する役割をもつ。Hsp90と相互作用するクライアントタンパク質にはプロテインキナーゼやステロイドホルモン受容体などの細胞増殖や分化に重要な役割を果たすシグナル伝達分子が多く含まれる³⁾。Hsp90はCdc37, p23やFKBP52といった他の分子シャペロン(コ・シャペロンと呼ぶ)と協働しながら、クライアントタンパク質が正しくシグナルに応答して機能するために必須の因子としてATP依存的に機能している^{4,5)}。特にHsp90のC最末端に認められるMEEVDモチーフは、多くのコ・シャペロンに認められるtetratricopeptide repeat (TPR) ドメインとの結合部位と考えられている³⁾。

3 TPRドメインを有するコ・シャペロン

TPRドメインを有するコ・シャペロンとして、HOP(Hsp90 and Hsp70 organizing protein), immunophilin(FKBP51, FKBP52, Cyp40), CHIPなどがある^{3,6)}。HOPには2カ所のTPRドメインが存在しており、そのためHsp70とHsp90に同時に会合することが可能になっている。これはクライアントタンパク質をHsp70からHsp90に受け渡すのに非常に都合が良い。また

HOPはHsp90のATPase活性を抑制して、クライアントタンパク質をHsp90にリクルートしやすくしている。

4 Hsp90のクライアントタンパク質と分子標的治療

Hsp90のクライアントタンパク質には変異型p53, ErbB2(Her2/neu), Bcr-Abl, HIF-1など、特にがん細胞の増殖や生存にかかわる機能タンパク質が多く含まれる。またエストロゲン受容体やアンドロゲン受容体などのステロイドホルモン受容体も主要なクライアントタンパク質であるが、乳がん、前立腺がんをはじめとしたホルモン依存性に増殖するがん細胞が多いことが知られている。このようにがん細胞はHsp90のクライアントタンパク質の機能に依存している‘addicted’の状態にあるといえる。このようなHsp90依存性のがん細胞においてoncogenicなクライアントタンパク質の機能を阻害することで抗がん剤として応用することが可能となる⁷⁾。

Hsp90阻害剤は、Hsp90のクライアントタンパク質のフォールディング不全を引き起こし、このようなクライアントタンパク質はユビキチン化を受け、プロテアソームによる分解が促進される。上述したように、Hsp90のクライアントタンパク質は非常に多くのタンパク質が知られており、Hsp90阻害剤は同時に多数のがん原性シグナル、例えば増殖、浸潤、抗アポトーシス、血管新生などを抑制できるため、非常に